

## 리튬판의 미세경도 온도 및 응력의존성

윤석영 · K.P.D. Lagerlof\*

부산대학교 무기재료공학과

\*CWRU 재료공학과

### Temperature and Load Dependence of the Microhardness of Rhenium Sheets

Seog-Young Yoon and K.P.D. Lagerlof\*

Department of Inorganic Materials Engineering at Pusan National University, 30 Changjung-Dong, Kumjung-Gu, Pusan, 607-735

\*Associate professor, Department of Materials Science and Engineering at Case Western Reserve University, Cleveland, OH 44106 USA

(2000년 1월 10일 받음, 2000년 3월 29일 최종수정본 받음)

초 록 리튬판의 미세경도를 압흔 하중 및 온도의 함수로 구하였다. 미세경도의 온도의존성은 상온에서 1000°C까지의 범위에서 Vickers 압흔기가 내장된 고온 미세압흔기를 이용하여 연구되었다. 미세경도의 하중의존성은 Vickers와 Knoop 압흔기를 이용하여 검토되었다. 압흔 크기 영향은 표준화된 Meyer's 법칙에 의해 충분히 설명되었다. 압흔도중 압흔기 아래에서의 가공경화 때문에 어닐링된 리튬판의 경도값은 높은 압흔 하중에서 압연된 리튬판의 경도값에 접근하였다. 경도의 하중의존성으로부터 외삽하여 얻어진 하중 영에서의 경도값은 높은 압흔 하중에서 압연된 리튬판의 경도값이 다른 열활성을 나타내는 두 개의 다른 기구에 의해 제어됨을 제시하였다. 낮은 온도에서 활성화에너지는 0.02eV였으며, 한편 높은 온도에서 활성화에너지는 0.15eV였다. 이때 전이온도는 대략 250°C이었다.

**Abstract** The microhardness of rhenium sheets was determined as a function of indentation load and temperature. The temperature dependence of the microhardness between room temperatures and 1000°C was studied using a hot microhardness tester equipped with a Vickers indenter. The load dependence of the microhardness was investigated using both a Vickers and a Knoop indenter. The indentation size effect (ISE) was well explained using the normalized Meyer's law. The hardness of the annealed rhenium sheet approached that of the as-rolled sheets at large indentation loads because of work-hardening under the indenter during indentation. The hardness at "zero load" (obtained from extrapolation of the load dependence of the hardness) suggested that the hardness is controlled by two different mechanisms having different thermal activation. At low temperature the activation energy for the mechanism controlling the hardness was approximately 0.02 eV, whereas at higher temperatures that was approximately 0.15 eV. The transition temperature between the two different controlling mechanisms was about 250°C.

**Key words** : cold working, hardness testing, mechanical properties

### 1. Introduction

Rhenium is an outstanding material for high temperature applications because of its high melting temperature ( $T_m = 3186^\circ\text{C}$ ), good high temperature mechanical strength, and creep properties.<sup>1,2)</sup> However, rhenium is often required to have a protective coating (e.g., Iridium) when used in oxidizing environments due to its poor oxidation properties.<sup>3)</sup> Rhenium foil with excellent formability at room temperature is normally produced by cold-working. However, the ductility is often limited to only a few percent deformation during high temperature annealing because of rapid work-hardening.<sup>4)</sup> Thus, a good understanding of the mechanical behavior of rhenium during deformation at room-temperature

and at elevated temperatures is needed to establish the optimum forming conditions. Several studies of the deformation and work-hardening behavior of rhenium have been carried out, including studies on the density change of rhenium sheets produced using traditional powder metallurgy during cold rolling.<sup>5,6)</sup>

Indentation hardness testing is a simple technique to assess the mechanical properties of materials. However, the most important concern in studying on microhardness indentation is the fact that the materials plastically deform during indentation. The nature of the indenter/sample interaction makes it difficult to properly assess the hardness of materials after different amounts of deformation. In recent years, there has been considerable interests in the nature of the hardness--

load dependence, where the hardness is measured as a function of indentation load.<sup>7-9)</sup> The indentation size effect (ISE) has been attributed to a variety of mechanisms taking a place in conjunction with the plastic deformation of material as well as indenter/sample interaction during indentation.

In the present work, the microhardness indentations on rhenium sheets were carried out at different temperatures and indentation loads to understand the dependence of temperature and indentation load on microhardness using a Vickers indenter. In addition, the microhardness indentations as a function of indentation load were carried out using a Knoop indenter to assess and examine the ISE better at room temperature.

## 2. Experimental procedure

### 2.1 Sample preparation

Two rhenium sheets were used to examine microhardness indentation in this study. One was the rhenium sheet produced from rhenium metal powder by pressing, pre-sintering and sintering, following by cold rolling (so called "as-deformed"). After cold rolling, rhenium sheet samples were deformed to about 30% strain in 5% deformation increments without intermediate annealing. The other was the rhenium sheet obtained from annealing at 1600°C for 20 minutes with deformed sheet (so called "annealed"). Both samples were cut from the rolled sheets into rectangular prisms (approximately 25mm × 4mm × 1.5mm) using a diamond saw, and the four major surfaces were polished using different grades of diamond paste, finishing with 1 μm grade and Syton (a colloidal silica slurry) to achieve a scratch-free mirror-like surface finish for the subsequent microhardness measurements.

### 2.2 Microhardness indentation

The microhardness of two samples at 50g load was measured between room temperature and 900°C at 50°C increments using a hot microhardness tester [Model QM, Nikon, Inc., Japan] operating at 10<sup>-5</sup> torr vacuum and equipped with a Vickers indenter. The load dependence of the microhardness was investigated using both a Vickers and a Knoop indenter. The Vickers indentations on rhenium sheets were carried out as a function of temperature, between room temperature and 1000°C in 100°C intervals, using the hot microhardness tester, whereas the Knoop indentations were obtained at room temperature using a Zwick hardness tester.

After indentation, the length of the two diagonals of the Vickers impression ( $d_1$  and  $d_2$ ) and the length of the long diagonal of the Knoop impression ( $L$ ) were im-

mediately measured using an optical microscopy [Nikon, Japan] equipped with precision micrometer eyepiece. Both the Vickers and Knoop hardness were calculated using formulae based on ASTM hardness numbers.<sup>10)</sup> However, instead of using conventional hardness numbers (having a dimension of  $Kgf/mm^2$ ), hardness values with the dimension  $Pa = N/m^2$  are used in this paper. Thus, the Vickers microhardness value was calculated using

$$H_v = C_v P/d^2 \quad (1)$$

where  $P$  is the load in *gram*,  $d$  is the average length of the indent diagonal in μm, and  $C_v = 18.2$  is a constant. Similarly, the Knoop microhardness value was calculated using

$$H_k = C_k P/L^2 \quad (2)$$

where  $L$  is the length of the long diagonal in μm, and  $C_k = 139.6$ . Microhardness values are reported as the averages of at least 10 indentation at each test load and temperature.

## 3. Results

### 3.1 Temperature dependence of the Vickers Microhardness

The temperature dependences of the Vickers microhardness using  $P=50g$  for the as-deformed and annealed samples are shown in Figure 1. Each data point represents the average of ten indents. As shown in Figure 1, the hardness of the as-deformed sample was slightly higher than that of the annealed sample in the overall temperature range. The hardness of both samples was almost constant up to 300°C from room temperature, however, decreased with increasing temperature above 300°C.

### 3.2 Indentation load dependence

Given the fact that the microhardness is load dependent because of plastic deformation at the vicinity of the indenter and indenter/sample interactions, it is important that the hardness is defined so that a consistent set of data (both with respect to temperature and indentation load) can be generated. Thus, Knoop microhardness using loads between 50 and 1500g at room temperature was examined to investigate the ISE. As shown in Figure 2, the measured hardness varies between approximately 10 GPa at 50g load and about 4 GPa at 1500g load. Furthermore, it can be seen that hardness is very load sensitive at small indentation

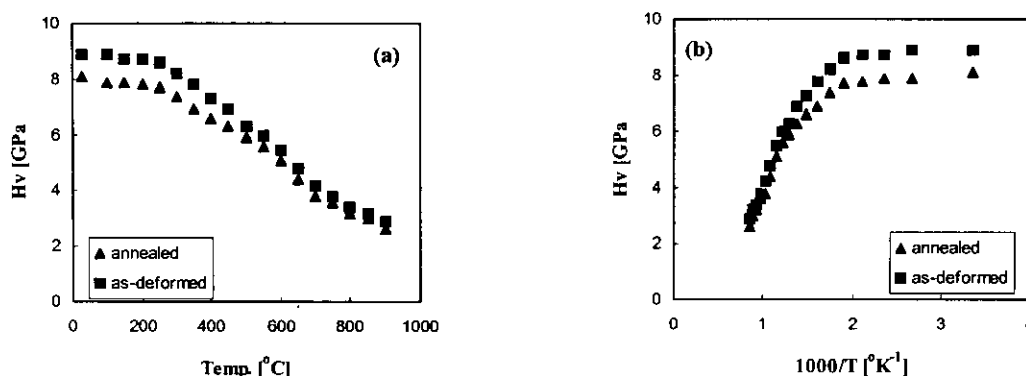


Fig. 1. Temperature dependence of Vickers microhardness of rhenium foil at a constant load 50g. (a) HV versus T [°C] (b) HV versus 1/T [K<sup>-1</sup>]

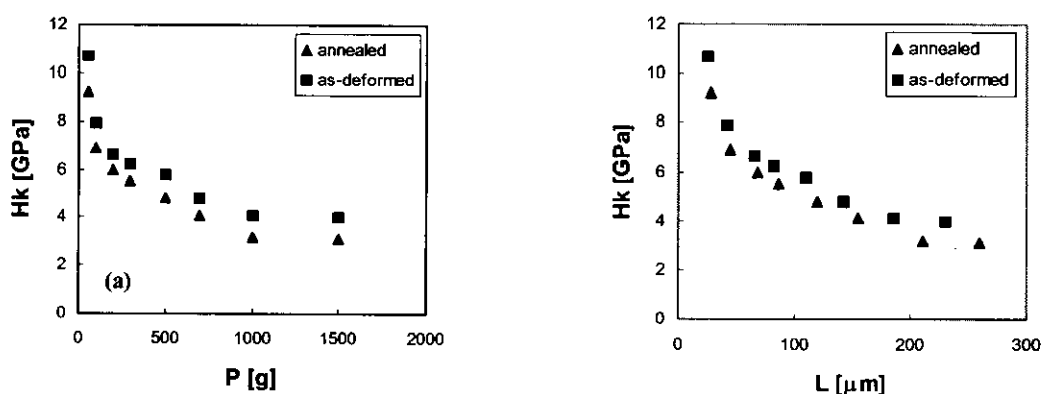


Fig. 2. Load (a) and indentation size (b) dependence of the Knoop microhardness of rhenium foil at room temperature.

Table 1. The temperature dependence of Vickers microhardness at zero load, H(0), P=50g load, H(50), and P=1000g load, H(1000), in as-deformed and annealed rhenium foil.

Temp. [°C]	Annealed			As-deformed		
	H(0) [GPa]	H(50) [GPa]	H(1000) [GPa]	H(0) [GPa]	H(50) [GPa]	H(1000) [GPa]
25	9.5	8.1	4.5	11.0	8.9	5.1
150	9.2	7.9	4.1	10.0	8.7	4.4
250	9.0	7.7	3.1	9.8	8.6	4.3
350	8.1	6.9	2.6	9.1	7.8	4.1
450	7.5	6.3	2.4	8.3	6.9	3.2
550	6.7	5.6	2.2	7.0	6.0	2.5
650	5.2	4.4	1.9	5.8	4.8	2.2
750	4.5	3.6	1.4	4.6	3.8	1.8
850	3.5	3.0	1.1	3.6	3.2	1.7
1000	2.3	2.0	1.0	2.4	2.4	1.4

loads<sup>11)</sup>, and becomes approximately constant at large loads (the load independent region).<sup>8-10)</sup>

### 3.3 Indentation load dependence as a function of temperature

The large and varying strain at the vicinity of the indents, as well as the significant indentation load dependence at room temperature, prompted concerns of whether the measured microhardness (determined as a function of temperature at a constant load of 50g

shown in Figure 1) represented hardness values from different regions of hardness-indentation load curves. Thus, the Vickers microhardness was determined as a function of load as well as temperature (Figure 3). It can be concluded that the Vickers microhardness is a significant function of load at all temperatures, especially at small indentation loads.

### 3.4 Hardness at zero and 1000g indentation loads

To provide a consistent definition of hardness, both

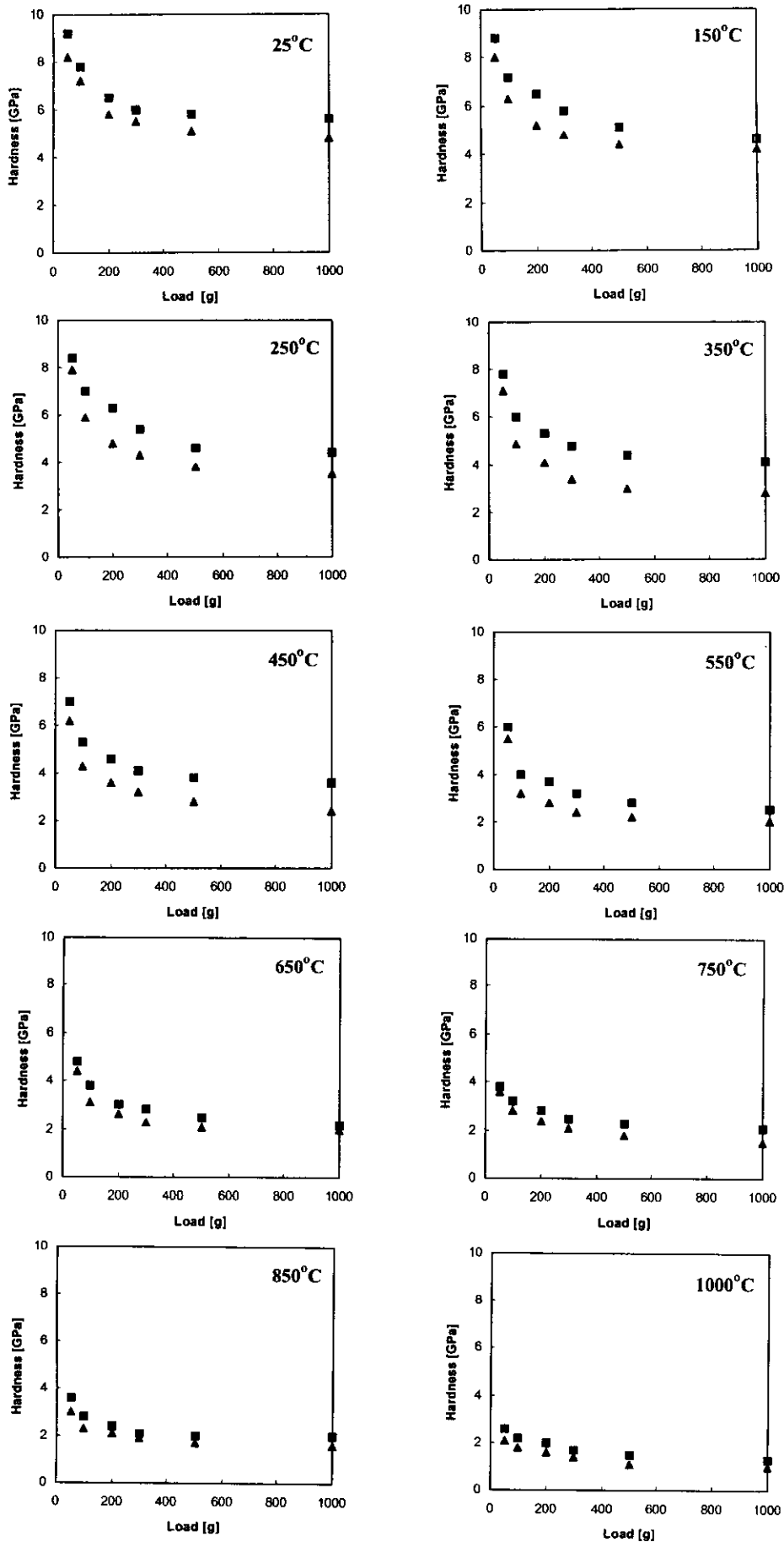


Fig. 3. Load dependence of Vickers microhardness of rhenium foil as a function of temperature.

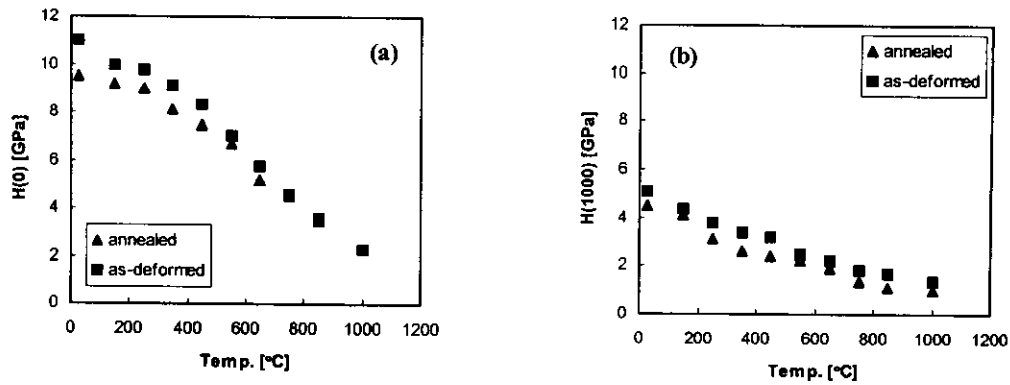


Fig. 4. Temperature dependence of Vickers microhardness. (a)  $H(0)$  versus  $T$  [ $^{\circ}\text{C}$ ] and (b)  $H(1000)$  versus  $T$  [ $^{\circ}\text{C}$ ].

with respect to indentation load and temperature, the extrapolated hardness at zero load,  $H(0)$ , and the hardness at 1000g load,  $H(1000)$ , were investigated (Table 1 and Figure 4).  $H(0)$  was calculated by fitting the measured microhardness in the load-dependent region to a polynomial function. This represents the hardness before any deformation is introduced by the indenter. Conversely,  $H(1000)$  corresponds to the hardness in the load-independent region at all temperatures, at which the deformation sub-structure introduced by the indenter is reasonably stable (or invariant to small changes of the indentation load).

#### 4. Discussion

##### 4.1 Microhardness load dependence

It is obvious from Figure 3 that the microhardnesses in both samples have a significant load-dependence at small loads. Thus, it is of importance to understand and model how the hardness is influenced by the applied load.

##### 4.1.1 The PSR model

Based on the observation that indentation-unloading curves are reasonably linear, Li and Bradt<sup>8)</sup> proposed a proportional specimen resistance model (PSR) to explain the indentation size effect. During Knoop microhardness indentation, the friction between a sample and an indenter would be proportional to the Knoop indentation size according to

$$PSR = a_1 L \tag{3}$$

The effective indentation test load would then be the applied indentation load minus the proportional specimen resistance ( $P_E = P - PSR$ ). Equating it to Kick's law [ $P_E = a_2 d^2$ ], the following relationship between the actual indentation load ( $P$ ) and indentation size ( $L$ ) is found

Table 2. The parameters  $a_1$  and  $a_2$  according to the PSR model in as-deformed and annealed rhenium foil.

Specimen	$a_1$ [ $\text{g}/\mu\text{m}$ ]	$a_2$ [ $\text{g}/\mu\text{m}^2$ ]
As-deformed	1.67	0.02
Annealed	1.77	0.02

$$P = a_1 L + a_2 d^2 \tag{4}$$

Here  $a_1$  is the Newtonian-like indenter/sample frictional resistance, and  $a_2$  is the Kick's law coefficient related to the true load-independent material hardness. Of interest is to note that when combining Eqs. (2) and (4), the hardness can be described as

$$H_K = C_k a_1 / L + C_k a_2 \tag{5}$$

where  $C_k a_2$  is the load-independent hardness obtained at large indentation size  $L$ .

In order to apply the PSR model as explaining the ISE of this materials in Figure 3, both the  $a_1$  and  $a_2$  values must be determined. These values can be obtained through the linear regression of  $P/L$  versus  $L$ . Such an analysis of the Knoop microhardness indentation results is shown in Figure 5, and the PSR fitting parameters are shown in Table 2. Although the fit assuming the PSR model shown in Figure 5 is relatively poor, the assumption that the load dependence of the microhardness at small loads can be fitted with a polynomial function is consistent with PSR model (at least as a first approximation).

##### 4.1.2 Meyer's law

A more general description of the ISE is provided by the so called Meyer's law<sup>12)</sup>

$$P = A d^n \tag{6}$$

or

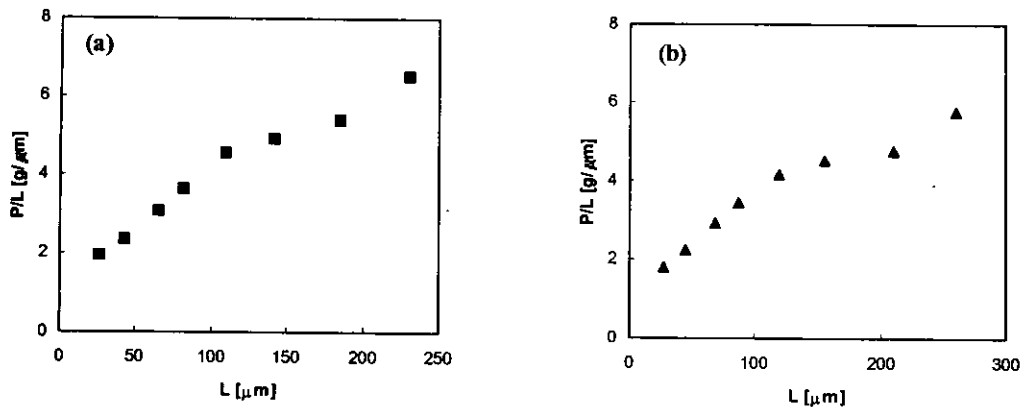


Fig. 5. The normalized indentation load ( $P/L$ ) as a function of indentation length ( $L$ ) according to the specimen resistance (PSR) (a) as-deformed and (b) annealed rhenium foil.

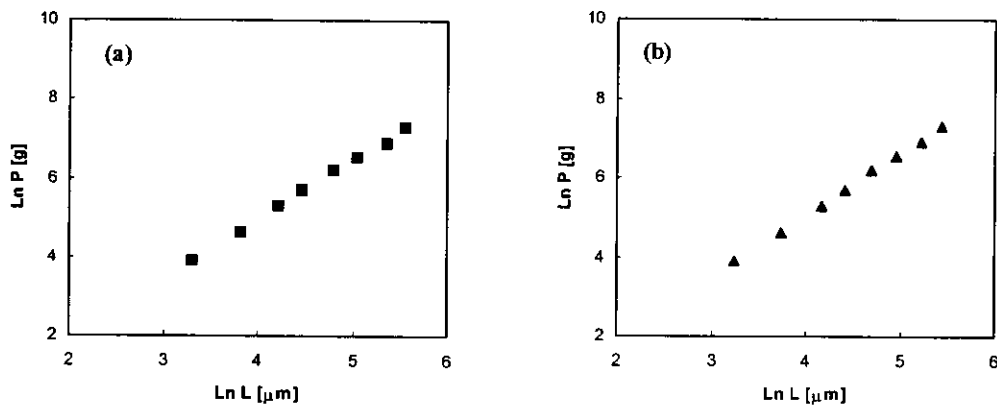


Fig. 6. The indentation load ( $\ln P$ ) as a function of indentation length ( $\ln L$ ) according to the Meyer's law (a) as-deformed and (b) annealed rhenium foil.

$$\ln P = \ln A + n \ln L \quad (7)$$

where  $A$  and  $n$  are empirical parameters. Using the results shown in Figure 2, plots assuming the logarithmic Meyer's law to describe the relationship between the indentation test load and indentation size are shown in Figure 6. With aid of regression analysis,  $A$  and  $n$  can readily be determined from the intercepts and the slopes of the lines in Figure 6, respectively, and are summarized in Table 3. The power exponent,  $n$ , was determined to be between 1 and 2, which resulted in a higher apparent microhardness at low indentation loads compared to that at higher indentation loads.

In order to alleviate the problems associated with the peculiar dimension of the constant  $A$  in Eq. (6), Li and Bradt<sup>13)</sup> suggested a normalized form of Meyer's law according to

$$P = 2P_c/n(L/L_c)^n \quad (8)$$

This equation defines the load-independent hardness through the constants  $P_c$  and  $L_c$ , which can be obtained

Table 3. Empirical parameters assuming Meyer's law for as-deformed and annealed rhenium foil.

Specimen	$A$	$n$
As-deformed	1.15	1.55
Annealed	1.09	1.51

from experimental results when the microhardness data is plotted as a function of the indentation test load and indentation size, respectively (as illustrated in Figure 5). However, in order to apply the normalized form of Meyer's law as according to Eq. (8), it is necessary to determine the load independent hardness,  $H_c$ , and the characteristic indentation size,  $L_c$ . According to Pollock *et al.*<sup>14)</sup> and Li *et al.*<sup>15)</sup>, an estimate of the load-independent hardness from the indentation size versus indentation load is given by

$$L = (14229/H_c)^{1/2} P^{1/2} - \alpha \quad (9)$$

where  $L$  and  $P$  have their original meaning according to Eq. (2), and  $\alpha$  is constant. The  $H_c$  value is the load-independent (or "true" hardness) characteristic of the high test load regime. When the indentation size ( $L$ )

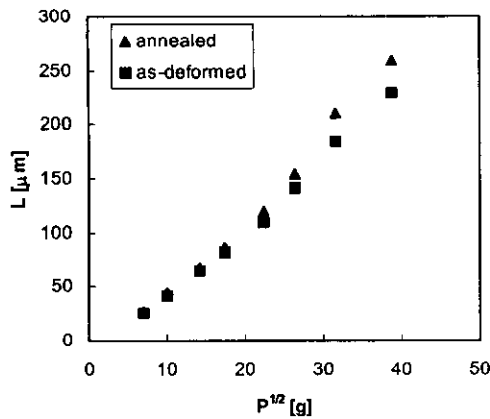


Fig. 7. The indentation length ( $L$ ) plotted as a function of  $P^{1/2}$  to estimate the load-independent hardness  $H_c$ , according to the normalized Meyer's law.

Table 4. Empirical parameters assuming the normalized Meyer's law for as-deformed and annealed rhenium foil.

Specimen	$H_c$ [GPa]	$L_c$ [ $\mu\text{m}$ ]	$P_c$ [g]
As-deformed	3.7	196	1030
Annealed	3.4	219	1175

was plotted as a function of  $P^{1/2}$ , this linear relationships became evident (as shown in Figure 7). The results are summarized in Table 4.

#### 4.2 Temperature dependence of the Vickers microhardness

Figure 3 shows that the microhardness decreases with increasing temperature, and the difference in hardness between the two samples at all temperatures is due to the fact that the deformation substructure, introduced during rolling, has changed in the annealed sample. Using the extrapolated hardness values at zero load,  $H(0)$ , and assuming that the deformation, introduced by the Vickers indenter, is thermally activated, the activation energy was approximately 0.02 eV between room temperature and 250°C, and 0.15 eV above 250°C. Both samples showed similar behaviors as a function of temperature, where the difference in hardness between the samples was a reflection of the retained deformation substructure. Studies of the deformation substructure, formed at vicinity of indents at different temperatures using transmission electron microscopy techniques, are underway. Such studies are expected to give a better understanding of the active deformation mechanisms at each temperature, and would provide information of any changes in the deformation controlling mechanism that may take place around 250°C. One possible explanation to the apparent change in thermal activation of the mechanism controlling the hardness would be that deformation twinning is

activated in addition to dislocation slip.

Of interest is to note that using hardness values, obtained at a load of 1000g,  $H(1000)$ , suggests that the hardness of the two samples are very different as a function of temperature. This behavior is interpreted as a demonstration of the difficulties to de-convolute the deformation micro-structure of the samples before indentation from that developed during indentation (in addition to other indenter-sample interactions).

## 5. Conclusions

The following conclusions can be drawn from the current investigation of the microhardness of as-deformed and annealed rhenium foils using Vickers and Knoop hardness indentation techniques as a function of indentation load and temperature.

1) The as-deformed rhenium foil is harder than the annealed foil at all temperatures. Thus, the deformation substructure is affected by the annealing after deformation. However, the difference in hardness is relatively small (especially at high temperatures). It can be suggested that a large amount of the deformation substructure remain after annealing.

2) The hardness at zero load,  $H(0)$ , represents a consistent definition of the hardness so that comparison of the hardness as a function of temperature can be made. Other definitions of the hardness can be used, although significant problems may arise in de-convoluting the work-hardening induced by the indenter during indentation from that of the specimen. This difficulty becomes even more significant when the hardness is studied at different temperatures (e.g., the hardness at 1000g load,  $H(1000)$ , displays a very complicated behavior as a function of temperature when the as-deformed sample is compared with the annealed sample).

3) It is evident that the ISE is affected by the sample/indenter interaction as well as details of the deformation substructure developed during indentation.

4) At low temperature, the thermal activation is very small (approximately 0.02 eV), whereas, at temperatures above 250°C, the activation energy is approximately 0.15 eV. This suggests that a change in the deformation mechanism controlling the measured hardness (i.e., the mechanism of plastic deformation) occurs at that temperature. One possible explanation of the apparent change around 250°C would be the onset of deformation twinning in addition to dislocation slip.

## References

1. B. D. Bryskin, *Advanced Materials and Processes*,

- September 22 (1992).
2. B. D. Bryskin, in *Proceedings of the Ninth Symposium on Space Nuclear Power Systems*, editors M. S. ElGenk and M. D. Hoover, pp.278-291 (American Institute of Physics, New York, 1992).
  3. J. C. Hamilton, N. Y. C. Yang, W. M. Clift, D. R. Boehme, K. F. McCarty and J. E. Franklin, *Met. Trans.*, **23A**, 851 (1992).
  4. E. M. Savitski, M.A. Tylkina, and K. B. Povarova, *Israel Program for Scientific Translations*, Jerusalem, pp.33-100 (1970).
  5. J. C. Carlen and B. Bryskin, *International J. of Refr. Met. and Hard Mater.*, **11** [6], 343-50 (1992).
  6. L. Larikov, M. Belyakova, and V. Rafalovski, *Cryst. Res. Technol.*, **26** [2], 239-44, (1991).
  7. H. Li, A. Ghosh, Y. H. Han, and R. C. Bradt, *J. Mater. Res.*, **8** [5], 1028-1032 (1993).
  8. H. Li and R. C. Bradt, *J. Mater. Sci.*, **28**, 917-926 (1993).
  9. H. Li and R. C. Bradt, *J. Non-crystalline Solids*, **146**, pp197-212 (1992).
  10. "Standard Test Methods for Microhardness of Materials," E384, *Annual Book of ASTM Standards*, Philadelphia, PA, pp.497-518, 1984.
  11. N. Gane and J. M. Cox, *Philos. Mag.*, **22**, 881 (1970).
  12. E. Meyer, *Phys. Z.*, **9**, 66 (1980).
  13. H. Li and R. C. Bradt, **A142**, 51 (1991).
  14. H. M. Pollock, D. Daugis and M. Baruins, in *Microindentation Techniques in Materials Science and Engineering*, edited P. J. Blau and B. R. Lawn, ASTM STP 889 (ASTM, Philadelphia, PA, 1984).
  15. S. Li, A. Ghosh, A. S. Kobayashi, and R. C. Bradt, *J. Am. Ceram. Soc.*, **72**, 904 (1989).